

A Steady-State Kinetic Model for Methanol Synthesis and the Water Gas Shift Reaction on a Commercial Cu/ZnO/Al₂O₃ Catalyst

K. M. Vanden Bussche¹ and G. F. Froment²

Laboratorium voor Petrochemische Techniek, Universiteit Gent, Krijgslaan 281, B9000 Gent, Belgium

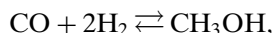
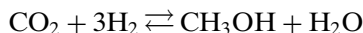
Received January 30, 1995; revised December 18, 1995; accepted January 30, 1996

A detailed reaction network, derived from literature data and our own experimental work, is used as a basis for the development of a steady-state kinetic model for methanol synthesis and the water gas shift reaction on a commercial Cu/ZnO/Al₂O₃ catalyst. Experimental data, obtained in a bench scale setup, operating between 180 and 280°C and at pressures up to 51 bar, are subsequently used for the estimation of the parameters in the proposed model. The result is a mechanistically sound kinetic model, comprising a set of statistically significant and physically meaningful parameter groups. It accurately predicts the experimentally obtained conversions, even upon extrapolation outside the originally applied experimental window. Using this model, the influence of inlet temperature, pressure, and the ratio of p_{CO} and p_{CO_2} are briefly illustrated. © 1996 Academic Press, Inc.

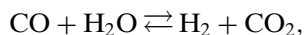
INTRODUCTION

The main lines in the mechanism of the conversion of a CO/CO₂/H₂ feed into methanol over a Cu/ZnO/Al₂O₃ catalyst are now well established, and a large number of kinetic equations have been proposed.

Generally speaking, the mechanism can be based on three overall reactions: the hydrogenations of CO₂ and CO,



with equilibrium constants K_1^* and K_2^* , and the water gas shift reaction,



with equilibrium constant K_3^* .

Early kinetic models were derived for the ZnO/Cr₂O₃ catalyst of the high pressure process, which has now almost completely been abandoned in favor of the low pressure

technology. A classic example from this early work is the equation proposed by Natta (1),

$$r_{\text{CH}_3\text{OH}} = \frac{f_{\text{CO}} f_{\text{H}_2}^2 - f_{\text{CH}_3\text{OH}}/K_2^*}{(A + Bf_{\text{CO}} + Cf_{\text{H}_2} + Df_{\text{CH}_3\text{OH}})^3},$$

in which f_i denotes the fugacity of component i and A , B , C , and D are estimated constants. Apparently, Natta assumed that only the hydrogenation of CO occurs, in which he proposed the trimolecular reaction of CO and molecular hydrogen to be rate determining.

Bakemeier *et al.* (2) noted an important discrepancy between their experimental observations on ZnO/Cr₂O₃ and Natta's predictions, particularly in the case of CO₂ rich feeds. For this reason, a CO₂ dependency was introduced in the equation in the shape of a Langmuir type isotherm. Assuming the methanol desorption to be rate determining, the authors ended up with

$$r_{\text{CH}_3\text{OH}} = \frac{Ae^{-E/RT} [p_{\text{CO}}^m p_{\text{H}_2}^n (1 - (p_{\text{CH}_3\text{OH}}/p_{\text{CO}} p_{\text{H}_2}^2 K_2^*))]}{1 + De^{-F/RT} p_{\text{CO}_2}/p_{\text{H}_2}},$$

whereby A , E , m , n , D , and F were determined from experimental data.

Leonov *et al.* (3) were the first to model methanol synthesis kinetics over a Cu/ZnO/Al₂O₃ catalyst. Their model again assumed CO to be the source of carbon in methanol and did not account for the influence of CO₂ in the feed:

$$r_{\text{CH}_3\text{OH}} = k \left(\frac{p_{\text{CO}}^{0.5} p_{\text{H}_2}}{p_{\text{CH}_3\text{OH}}^{0.66}} - \frac{p_{\text{CH}_3\text{OH}}^{0.34}}{p_{\text{CO}}^{0.5} p_{\text{H}_2} K_2^*} \right).$$

Andrew (4) used a power law type of equation, with an extra Φ_{CO_2} function to account for the occurrence of a maximum in the carbon conversion to methanol when adding CO₂ to the CO/H₂ feed.

Whereas these first authors used a more or less correlative approach, a number of later contributions focused on effectively implementing detailed mechanistic considerations in the kinetic model.

¹ Present address: Koninklijke/Shell Laboratorium, P.O. Box 38000, NL-1030BN Amsterdam, The Netherlands. E-mail: busschel@ksla.nl.

² To whom correspondence should be addressed.

Klier *et al.* (5) no longer considered CO to be the only, but still the most important source of carbon in methanol. Experimental variation of the $p_{\text{CO}}/p_{\text{CO}_2}$ ratio, at a fixed total pressure and hydrogen concentration revealed a maximum in the synthesis rate. They ascribed the decrease of the reaction rate at low $p_{\text{CO}}/p_{\text{CO}_2}$ to a strong adsorption by CO_2 , while at high ratios an excessive reduction of the catalyst was thought to take place. The ratio of the number of active, oxidized sites and the inactive, reduced sites is solely determined by the $p_{\text{CO}}/p_{\text{CO}_2}$, through a redox-like mechanism, the equilibrium of which is characterized by K_{redox} . They further assumed competitive adsorption of CO_2 and CO or H_2 , and accounted for the direct hydrogenation of CO_2 by an empirical term. This led to the equation

$$r_{\text{CH}_3\text{OH}} = \text{const} \frac{K_{\text{redox}}^3 (p_{\text{CO}_2}/p_{\text{CO}})^3 (p_{\text{CO}} p_{\text{H}_2}^2 - p_{\text{CH}_3\text{OH}}/K_2^*)}{[1 + K_{\text{redox}} (p_{\text{CO}_2}/p_{\text{CO}})]^3 (F + K_{\text{CO}_2} p_{\text{CO}_2})^n} + k' (p_{\text{CO}_2} - (1/K_1^*) (p_{\text{CH}_3\text{OH}} p_{\text{H}_2\text{O}}/p_{\text{H}_2}^3)).$$

These equations later served as a base for the work of McNeil *et al.* (6), who expanded on the mechanism of the direct hydrogenation of CO_2 and the possible role of ZnO as a hydrogen reservoir. Despite the much larger number of parameters in the resulting model, the latter authors did not manage to show a significantly better agreement between the experimental and the simulated results than that already obtained by Klier *et al.* (5).

Villa *et al.* (7) realized that a thorough modeling of the methanol synthesis system should also involve a description of the water gas shift reaction. Assuming thereby again that the hydrogenation of CO is the only route to methanol, this resulted in the following set of equations

$$r_{\text{CH}_3\text{OH}} = \frac{f_{\text{CO}} f_{\text{H}_2}^2 - f_{\text{CH}_3\text{OH}}/K_2^*}{(A + B f_{\text{CO}} + C f_{\text{H}_2} + G f_{\text{CO}_2})^3}$$

$$r_{\text{RWGS}} = \frac{f_{\text{CO}_2} f_{\text{H}_2} - f_{\text{CO}} f_{\text{H}_2\text{O}} K_3^*}{M^2},$$

implying that the generation of methanol and the water gas shift occur on different types of sites.

Graaf *et al.* (8, 9) considered both the hydrogenation of CO and CO_2 as well as the water gas shift reaction. Inspired by the work of Herman *et al.* (10), the authors proposed a dual site mechanism, adsorbing CO and CO_2 on an s_1 type site and H_2 and water on a site s_2 . Formation of methanol from CO and CO_2 occurs through successive hydrogenations, while the water gas shift reaction proceeds along a formate route. Assuming the ad- and desorptions to be in equilibrium and taking every elementary step in each of the three overall reactions in its turn as rate determining, the authors ended up with 48 possible models. Statistical discrimination allowed them to select the following final set of

equations:

$$r_{\text{CH}_3\text{OH},1} = \frac{k'_{\text{ps},1c} K_{\text{CO}_2} [f_{\text{CO}_2} f_{\text{H}_2}^{3/2} - f_{\text{CH}_3\text{OH}} f_{\text{H}_2\text{O}} / (f_{\text{H}_2}^{3/2} K_1^*)]}{(1 + K_{\text{CO}} f_{\text{CO}} + K_{\text{CO}_2} f_{\text{CO}_2}) [f_{\text{H}_2}^{1/2} + (K_{\text{H}_2\text{O}}/K_{\text{H}_2}^{1/2}) f_{\text{H}_2\text{O}}]}$$

$$r_{\text{CH}_3\text{OH},2} = \frac{k'_{\text{ps},2c} K_{\text{CO}} [f_{\text{CO}} f_{\text{H}_2}^{3/2} - f_{\text{CH}_3\text{OH}} / (f_{\text{H}_2}^{1/2} K_2^*)]}{(1 + K_{\text{CO}} f_{\text{CO}} + K_{\text{CO}_2} f_{\text{CO}_2}) [f_{\text{H}_2}^{1/2} + (K_{\text{H}_2\text{O}}/K_{\text{H}_2}^{1/2}) f_{\text{H}_2\text{O}}]}$$

$$r_{\text{RWGS}} = \frac{k'_{\text{ps},3b} K_{\text{CO}_2} (f_{\text{CO}_2} f_{\text{H}_2} - f_{\text{H}_2\text{O}} f_{\text{CO}} K_3^*)}{(1 + K_{\text{CO}} f_{\text{CO}} + K_{\text{CO}_2} f_{\text{CO}_2}) [f_{\text{H}_2}^{1/2} + (K_{\text{H}_2\text{O}}/K_{\text{H}_2}^{1/2}) f_{\text{H}_2\text{O}}]}.$$

In doing this, however, the authors failed to account for the fact that some intermediates feature in two different overall reactions. This implies that the model simultaneously predicts two different concentrations of one and the same intermediate like formyl and methoxy species.

Parallel to this evolution, Russian groups led by Rozovskii and Temkin (see references to this work in (11)) developed a number of kinetic models for the SNM type Cu/ZnO/Al₂O₃ catalysts. Since neither of these groups ever succeeded in producing methanol from a dry mixture of CO and hydrogen, the models are all based on the direct hydrogenation of CO_2 to methanol, while the majority also accounts for the occurrence of the water gas shift reaction. Malinovskaya *et al.* (11) compared a number of these models using own experimental data and selected the following set of equations, originally presented by Mochalin *et al.* (12):

$$r_{\text{CH}_3\text{OH}} = \frac{k_1 p_{\text{CO}_2} p_{\text{H}_2} (1 - p_{\text{CH}_3\text{OH}} p_{\text{H}_2\text{O}} / (K_1^* p_{\text{CO}_2} p_{\text{H}_2}^3))}{p_{\text{CO}_2} + K_{\text{H}_2\text{O}} p_{\text{CO}_2} p_{\text{H}_2\text{O}} + K'' p_{\text{H}_2\text{O}}}$$

$$r_{\text{RWGS}} = \frac{k_2 p_{\text{H}_2} p_{\text{CO}_2} (1 - p_{\text{CO}} p_{\text{H}_2\text{O}} K_3^* / (p_{\text{CO}_2} p_{\text{H}_2}))}{p_{\text{CO}_2} + K_{\text{H}_2\text{O}} p_{\text{H}_2\text{O}} p_{\text{CO}_2} + K'' p_{\text{H}_2\text{O}}}$$

Unfortunately, the authors did not expand on the physical background of the model, nor did they mention the numerical value of the different parameters in the model.

In the current work, a detailed reaction scheme for the conversion of syngas over a Cu/ZnO/Al₂O₃ catalyst will be proposed, serving as the backbone for the development of a mechanistically sound kinetic model. It will account for the hydrogenation to methanol and include the reverse water gas shift.

EXPERIMENTAL

Figure 1 presents a schematic view of the bench scale setup that was used for the acquisition of the kinetic data. In the feed section, the reactants CO, CO_2 , and H_2 and the internal standard argon were led through a set of mass flow

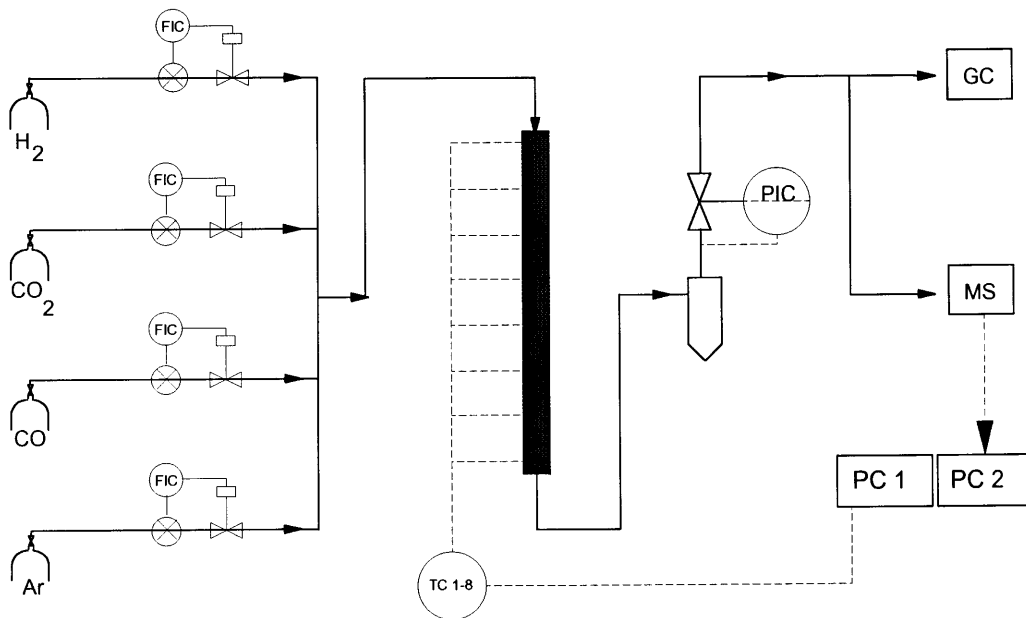


FIG. 1. Schematic view of the bench scale reactor system used in the kinetic data acquisition.

controllers (Brooks 5850TR). The use of pure CO₂ ensures flexibility in the choice of the feed composition, but also sets an upper limit for the operating pressure, since CO₂ condenses at 54 bar at ambient temperature.

The stainless steel reactor was of the tubular type, with an internal diameter of 15.8 mm and a length of 150 mm, withstanding temperatures up to 400°C and pressures of 100 bar, governed by a membrane back pressure controller. An insulating cover (Fiberfrax Duraboard 1200 by Carborundum) minimized radial and axial heat losses. The reactor was divided into three heating zones, each with its own PID temperature controller (Shinoh MCS), facilitating isothermal operation. The temperature profile along the bed was measured by means of eight thermocouples (TC), situated at the central axis of the reactor. The TC are linked to a PC, enabling a continuous and on line registration of the temperature profile.

The experiments involved a commercial ICI 51-2 Cu/ZnO/Al₂O₃ catalyst, ground into 0.125- to 0.25-mm or 0.3- to 0.7-mm particles. It was diluted with an inert, for the sake of isothermicity, and positioned in the reactor between a top and a bottom inert bed. The height of the bed in most cases amounted to about 5 cm. Since the reactor diameter was 16 mm and the pellet size never surpassed 0.7 mm, the ratio d_r/d_p always exceeded 22, ensuring a uniform distribution of the feed over the reactor section (13).

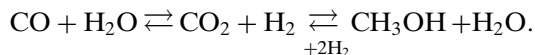
The high-pressure effluent lines, containing water and methanol, were constantly kept at temperatures above 150°C, by means of Habia electrical resistance heat wiring, to avoid condensation. The gas finally reached the analysis section, where a gas chromatograph (GC, Packard 438S)

determined its composition, while a mass spectrometer (Balzers 420), scanning the concentration of the different gas phase species in time, revealed possible disturbances in the intended steady-state reactor operation.

Due to the limited sensitivity of the GC katharometer, the reactor was operated in an integral fashion (13), yielding the conversions of the different reactants as experimental responses. The absence of diffusional limitations, internal as well as external, was thoroughly verified using methods described by Froment and Bischoff (13).

REACTION MECHANISM AND DERIVATION OF THE KINETIC EQUATIONS

Based on the results of Chinchén *et al.* (14) and Rozovskii (15), we assume that CO₂ is the main source of carbon in methanol. A thorough description of this reaction system should also account for the water gas shift, proceeding along a redox mechanism (16–20):



Both reactions proceed on the copper phase of the catalyst (16). The role of ZnO is limited to structural promotion, at least under the typical industrial conditions applied in the current paper (21). A mechanism, occurring exclusively and completely on the copper phase, is proposed in Fig. 2.

Both H₂ and CO₂ adsorb dissociatively on the copper surface. The oxidizing adsorption of CO₂ on metallic copper is promoted by traces of surface oxygen or alkaline

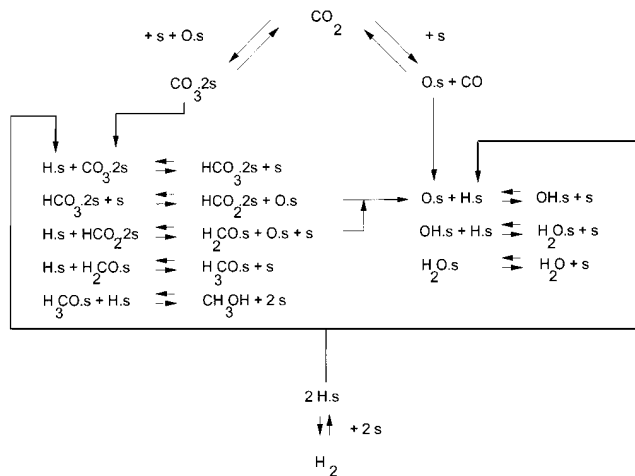


FIG. 2. Reaction scheme for the synthesis of methanol and the water gas shift reaction.

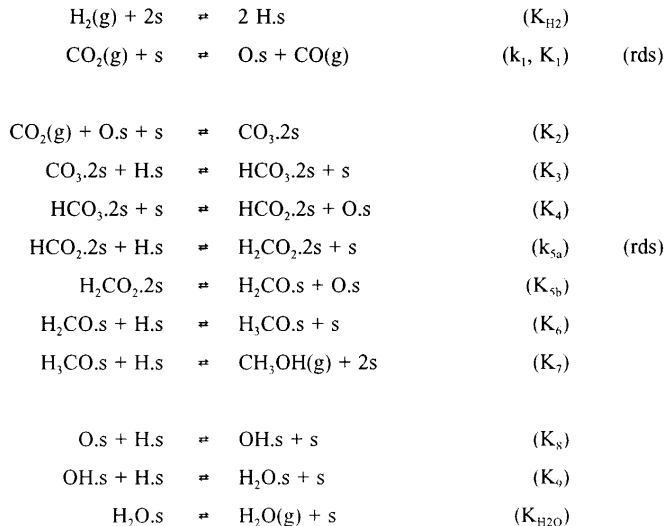
species (22–25). On the oxidized copper surface, carbonate structures are formed by further adsorption of CO_2 (26–28). These carbonates are quickly hydrogenated, first to bicarbonate structures and subsequently to Cu formate, formaldehyde, methoxy species, and finally methanol. In this sequence, shown in the left-hand side of Fig. 2, the rate determining step is the hydrogenation of the formate, which is generally accepted to be the longest living intermediate in methanol synthesis on copper (15, 20, 29).

At two stages in the hydrogenation of CO_2 to methanol, surface oxygen is released from the molecule. This species is also hydrogenated by the available hydrogen atoms, yielding hydroxyl groups and subsequently water, which is known to desorb relatively slowly. In fact, the right-hand side of Fig. 2 describes the reverse water gas shift reaction, proceeding according to a redox mechanism. In this sequence of reactions, the dissociative adsorption of CO_2 is rate determining, as was shown by Nakamura *et al.* (17), Fujita *et al.* (30), and Ernst *et al.* (31). Their results, for equimolar mixtures of CO_2 and H_2 , are all the more valid under industrial conditions, since the ratio $p_{\text{CO}_2}/p_{\text{H}_2}$ then only amounts to 0.05.

Scheme I shows the different elementary reaction steps to be considered and introduces the nomenclature for the equilibrium (K_i) and rate (k_i) constants.

Derivation of the corresponding set of kinetic equations is performed under the hypothesis of pseudo-steady-state of the concentration of the different surface intermediates (13). The concentration of free active sites, c_s , can be obtained from a balance over the total number of sites, c_t , from which the concentrations of the surface intermediates have been eliminated. This balance for c_t is given by

$$1 = \frac{c_s}{c_t} + \frac{c_{\text{O.s}}}{c_t} + \frac{c_{\text{H}_2\text{O},2\text{s}}}{c_t} + \frac{c_{\text{HCO}_2,2\text{s}}}{c_t} + \frac{c_{\text{CO}_3,2\text{s}}}{c_t} + \frac{c_{\text{H.s}}}{c_t}.$$



SCHEME I. Reaction scheme for the synthesis of methanol and the reverse water gas shift reaction. rds, rate determining step.

Note that the concentrations of adsorbed bicarbonate, formaldehyde, methoxy, methanol, and hydroxyl species were not taken into account, since their concentration is negligible under reaction conditions (16–18, 28, 31).

The determination of c_s is somewhat complicated by the bridging adsorption of CO_2 . Indeed, upon elimination of the surface species concentrations, the balance becomes

$$1 = b \cdot \frac{c_s}{c_t} + a \cdot \left(\frac{c_s}{c_t} \right)^2,$$

in which

$$\begin{aligned} a &= K'_2 K_3 K_4 \sqrt{K_{\text{H}_2}} p_{\text{CO}_2} \sqrt{p_{\text{H}_2}} + \frac{K'_2 K_{\text{H}_2\text{O}}}{K_{\text{H}_2} K_8 K_9} \frac{p_{\text{H}_2\text{O}} p_{\text{CO}_2}}{p_{\text{H}_2}}, \\ b &= 1 + \frac{K_{\text{H}_2\text{O}}}{K_8 K_9 K_{\text{H}_2}} \frac{p_{\text{H}_2\text{O}}}{p_{\text{H}_2}} + \sqrt{K_{\text{H}_2} p_{\text{H}_2} + K_{\text{H}_2\text{O}} p_{\text{H}_2\text{O}}}, \end{aligned} \quad [1]$$

and

$$K'_2 = K_2 \cdot c_t.$$

This balance is not linear in c_s and has to be solved as a quadratic equation in c_s/c_t . Only the positive root has to be considered. Simple analysis reveals that the normalized concentration of free active sites,

$$\beta = \frac{c_s}{c_t} = \frac{-b + \sqrt{b^2 + 4a}}{2a}, \quad [2]$$

always lies between 0 and 1, as is physically expected.

Upon introduction of the rate determining steps and elimination of the concentration of the surface intermedi-

ates, the following expressions are obtained for the rate of methanol synthesis and the reverse water gas shift reaction

$$r_{\text{MeOH}} = k'_{5a} K'_2 K_3 K_4 K_{\text{H}_2} p_{\text{CO}_2} p_{\text{H}_2} \left(1 - \frac{1}{K_1^*} \frac{p_{\text{H}_2\text{O}} p_{\text{CH}_3\text{OH}}}{p_{\text{H}_2}^3 p_{\text{CO}_2}} \right) \beta^3$$

$$r_{\text{RWGS}} = k'_1 p_{\text{CO}_2} \left(1 - K_3^* \frac{p_{\text{H}_2\text{O}} p_{\text{CO}}}{p_{\text{CO}_2} p_{\text{H}_2}} \right) \beta,$$

in which

$$k'_{5a} = k_{5a} \cdot c_t^2$$

$$k'_1 = k_1 \cdot c_t,$$

and β represents a function of partial pressures and parameter groups, given by [1] and [2]. The use of fugacities, rather than partial pressures, was considered, applying the Soave–Redlich–Kwong equation of state (36). The compressibility factors were never outside the 0.99 to 1.01 range and found to give negligible changes in the results.

The equilibrium constants K_1^* and K_3^* are thermodynamically determined. The values were taken from Graaf *et al.* (1986):

$$\log_{10} k_1^* = \frac{3066}{T} - 10.592$$

$$\log_{10} 1/K_3^* = \frac{-2073}{T} + 2.029.$$

PARAMETER ESTIMATION

As mentioned under Experimental, the kinetic data were obtained in an integral reactor, and, therefore, require integration of the conservation equations over the reactor. In the current context, a pseudohomogeneous one-dimensional model was applied (13). In view of the fact that the (isothermal) temperature profile was determined experimentally, integration of the energy equation was not necessary, while the pressure drop was also negligible. Under steady-state conditions, two independent responses completely describe the system, so that only two continuity equations (e.g., for CO and CO₂) had to be considered. The integration of the two equations, containing the proposed kinetic expressions, was performed applying fourth- and fifth-order Runge Kutta methods.

The parameter estimation was based on minimization of

$$\sum_{i=1}^2 w_i \sum_{j=1}^n (y_{ij,\text{obs}} - y_{ij,\text{calc}})^2,$$

where n is the total number of experiments and w_i stands for the weight factor for response i . The latter is inversely proportional to the variance of the response, derived from a set of replicate experiments. The actual minimization of

this object function made use of a Levenberg–Marquardt routine of the multiresponse type (33).

Values were determined for the frequency and exponential factors of the parameter groups

$$\sqrt{K_{\text{H}_2}}, \quad K_{\text{H}_2\text{O}}, \quad K'_2 K_3 K_4 \sqrt{K_{\text{H}_2}}, \quad \frac{K_{\text{H}_2\text{O}}}{K_8 K_9 K_{\text{H}_2}},$$

$$\frac{K'_2 K_{\text{H}_2\text{O}}}{K_8 K_9}, \quad k'_{5a} K'_2 K_3 K_4 K_{\text{H}_2}, \quad k'_1,$$

so the number of parameters to be estimated amounted to 14.

This was done using a total of 276 experiments,³ each yielding two responses. The temperature was varied between 180 and 280°C, and the pressure from 15 to 51 bar. The ratio $p_{\text{CO}}/p_{\text{CO}_2}$ ranged from 0 to 4.1.

In the subsequent calculations, the groups describing the surface concentration of carbonates and formate,

$$K'_2 K_3 K_4 \sqrt{K_{\text{H}_2}}$$

and

$$\frac{K'_2 K_{\text{H}_2\text{O}}}{K_{\text{H}_2} K_8 K_9},$$

never yielded any statistically significant contribution. The surface converge by these species was, therefore, considered to be negligible and discarded from the β factor. By leaving out these bridging compounds, however, the a term in equation [1] becomes identical to 0 and the normalized concentration of free active sites β is reduced to

$$\frac{1}{1 + (K_{\text{H}_2\text{O}}/K_8 K_9 K_{\text{H}_2})(p_{\text{H}_2\text{O}}/p_{\text{H}_2}) + \sqrt{K_{\text{H}_2} p_{\text{H}_2}} + K_{\text{H}_2\text{O}} p_{\text{H}_2\text{O}}}.$$

The form of the kinetic expressions for methanol synthesis and the reverse water gas shift reaction remains unchanged, provided that the modified β is used.

The parameter values eventually obtained are given in Table 1. Since a reparametrisation was applied in the estimation, the numbers pertain to the formula

$$\kappa(i) = A^*(i) \exp\left(-\frac{B(i)}{R} \left(\frac{1}{T_{\text{av}}} - \frac{1}{T}\right)\right),$$

in which T_{av} equals 501.57 K.

Calculating the frequency factors back to the original context of Arrhenius or Van't Hoff,

$$A(i) \exp(B(i)/RT),$$

where $B(i)$ represents either E or $(-\Delta H)$ or a combination of those, the parameter values of Table 2 are obtained,

³ The data set was too extensive to be incorporated in full in the text. It is available from the corresponding author.

TABLE 1
Parameter Values and Corresponding Approx. 95% Confidence Intervals for the Kinetic Model

κ		Value	Standard deviation	Lower limit 95% conf. int.	Upper limit 95% conf. int.	$t_{0.95}$ value
$\sqrt{K_{H_2}}$	A*	30.82	0.375	30.08	31.56	81.97
	B	17,197	1864	13,545	20,850	9.23
K_{H_2O}	A*	558.17	10.18	538.23	578.11	54.86
	B	124,119	3058	118,125	130,112	40.59
$\frac{K_{H_2O}}{K_8 K_9 K_{H_2}}$	A*	3,453.38	260.29	2,943.21	3,963.55	13.27
	B	—	—	—	—	—
$\frac{k'_{5a} K'_2 K_3}{K_4 K_{H_2}}$	A*	7,070.34	259.75	6,561.23	7,579.45	27.22
	B	36,696	6102.8	24,734	48,657	6.01
k'_1	A*	1.65	0.02	1.61	1.69	82.31
	B	-94,765	1694	-98,084	-91,446	-55.96

which are introduced in

$$r_{MeOH} = \frac{k'_{5a} K'_2 K_3 K_4 K_{H_2} p_{CO_2} p_{H_2} [1 - (1/K^*) (p_{H_2O} p_{CH_3OH} / p_{H_2}^3 p_{CO_2})]}{(1 + (K_{H_2O} / K_8 K_9 K_{H_2}) (p_{H_2O} / p_{H_2}) + \sqrt{K_{H_2} p_{H_2} + K_{H_2O} p_{H_2O}})^3}$$

$$r_{RWGS} = \frac{k'_1 p_{CO_2} [1 - K_3^* (p_{H_2O} p_{CO} / p_{CO_2} p_{H_2})]}{(1 + (K_{H_2O} / K_8 K_9 K_{H_2}) (p_{H_2O} / p_{H_2}) + \sqrt{K_{H_2} p_{H_2} + K_{H_2O} p_{H_2O}})^3} \quad [3]$$

in which the pressures are expressed in bar and the reaction rates in mol/kg_{cat}/s.

EVALUATION OF THE MODEL

Three criteria are used to evaluate the model. First of all, the agreement between the calculated and experimentally obtained conversions is checked. Second, closer attention is paid to the statistical significance and the physico-chemical meaning of the parameters. Finally, the model response to

variations of the operating conditions, both in- and outside the experimentally applied window, is analyzed.

The parity plots for the fractional conversion of CO and CO₂ are given in Figs. 3 and 4. The agreement is excellent over the complete range of conversions. The deviations from the diagonal are random and do not show any trends. Analysis of the parity plots for individual temperatures and pressures confirms the absence of systematic errors.

In this context, the statistical significance of the regression was also checked. Due to the nonlinear aspects of the model, the customary *F* test (comparing the sum of squares due to regression to the residual sum of squares, corrected for their respective degrees of freedom) is only indicative, but the obtained *F* value of 11,418 is three orders of magnitude larger than the tabulated 99% value, which is 2.56.

Besides the parameter values, Table 1 also shows the approximate 95% confidence intervals and the corresponding $t_{0.95}$ values. Again, these values are approximate, since the

TABLE 2
Parameter Values for the Steady-State Kinetic Model

$\sqrt{K_{H_2}}$	A	0.499
	B	17,197
K_{H_2O}	A	6.62×10^{-11}
	B	124,119
$\frac{K_{H_2O}}{K_8 K_9 K_{H_2}}$	A	3,453.38
	B	—
$\frac{k'_{5a} K'_2 K_3}{K_4 K_{H_2}}$	A	1.07
	B	36,696
k'_1	A	1.22×10^{10}
	B	-94,765

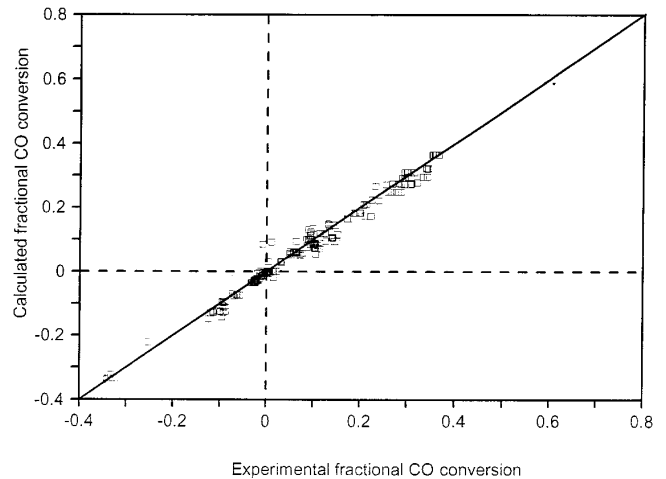


FIG. 3. Parity plot for the fractional conversion of CO.

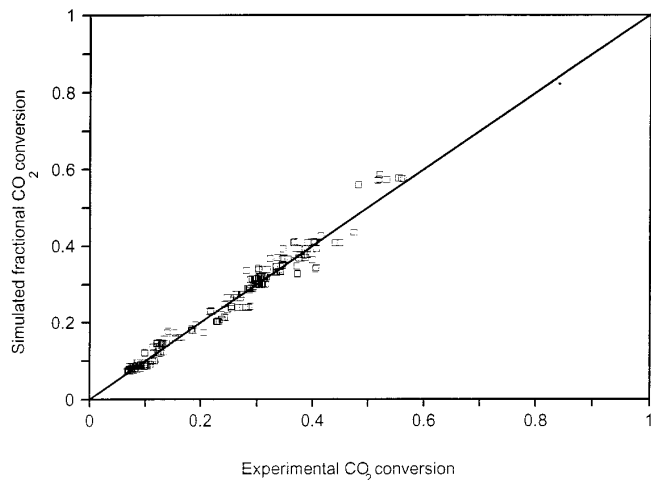


FIG. 4. Parity plot for the fractional CO₂ conversion.

model is not linear in the parameters. The tabulated $t_{0.95}$, with 543 degrees of freedom, amounts to 1.96. This value is amply exceeded by all parameters, indicating that each of them is significantly nonzero, with an approximate probability of 95%

Upon recalculation of the frequency factors to the original Arrhenius or Van't Hoff equations, all parameters stay significantly different from 0 with a 95% probability, except for the frequency factor of the water adsorption constant. Due to correlation between the heat of adsorption and the frequency factor, the probability of the latter fulfilling a significant role in the model is reduced to 90%.

The parameters also have to obey a number of physico-chemical constraints, as stipulated by Boudart (34). Since parameters 3 and 4 of Table 1 are lumps of physical constants, they are only partly bound by these rules.

A first criterion, which is perfectly satisfied in the current case, specifies that all frequency factors have to be positive. Furthermore, if the parameter describes an adsorption constant, the frequency factor is subject to two additional rules, since it then physically represents $e^{\Delta S^{\circ}_{\text{ads}}/R}$. This ($-\Delta S^{\circ}$) has to remain positive and should not exceed the entropy of the gas S° at this temperature:

$$0 \leq -\Delta S^{\circ}_{\text{ads}} \leq S^{\circ}.$$

Parameter 1, describing the square root of the hydrogen adsorption constant, satisfies both criteria, since $-\Delta S^{\circ}_{\text{ads}}$ and S° respectively amount to 11.56 and 145 J/mol/K. The water adsorption constant, i.e., parameter 2, also passes the test, with values of 195 and 207 J/mol/K, respectively (S° values taken from Stull *et al.* (35)).

A third and final rule pertains to the sign of $B(i)$. It has to be positive for the adsorption constants, reflecting the heat of adsorption. Parameters 1 and 2 satisfy this criterion. The exponential of the reaction rate constants on the other

TABLE 3

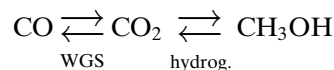
Operating Conditions for the Simulation of the Bench Scale Reactor

Catalyst	
Density (kg/m ³)	1775
Porosity (m ³ /m ³)	0.5
Mass (g)	34.8
Pellet diameter (m _s)	0.0005
Reactor	
Diameter (m _r)	0.016
Length (m _r)	0.15
Operating conditions	
T° (K)	493.2
p_1° (bar)	50
m (10 ⁻⁵ kg/s)	2.8
Feed composition	
CO (mol%)	4.00
H ₂ O (mol%)	0.00
MeOH (mol%)	0.00
H ₂ (mol%)	82.00
CO ₂ (mol%)	3.00
Inert (mol%)	11.0

hand has to be negative, since it stands for $-E_a$. Parameter 5 successfully passes this criterion.

Finally, the model response to variations in the operating conditions is tested. This is done by simulation of an adiabatic bench scale reactor. The catalyst pellets are taken sufficiently small, to avoid blurring of the results by diffusion-related effects. The conditions are summarized in Table 3.

Figure 5 shows the simulated concentration and temperature profiles along the reactor for the base case. The interpretation will adopt the following simplified reaction sequence:



Initially, CO₂ reacts to give CO as well as methanol. Since the reverse water gas shift is endothermic, and because of the decreasing CO₂ concentration, this slows down the hydrogenation of CO₂ at the reactor inlet. At 3 mm into the bed the reverse water gas shift reaches its equilibrium value and subsequently switches direction. This results in an inflection point in the temperature profile and the concentration evolution of water and methanol. From this point onward, the reactions are strictly in series. At 3 cm in the bed, the thermodynamic equilibrium concentrations are attained.

The effect of varying the inlet pressure is shown in Fig. 6. Since the production of methanol causes a decrease in the number of moles, the reaction is favored by elevated pressures. A pressure increase results in higher exit concentrations of methanol (Fig. 6a) and, in view of the exothermicity of the reaction, also in a higher exit temperature (Fig. 6b). The increased gradient of the temperature profile at higher

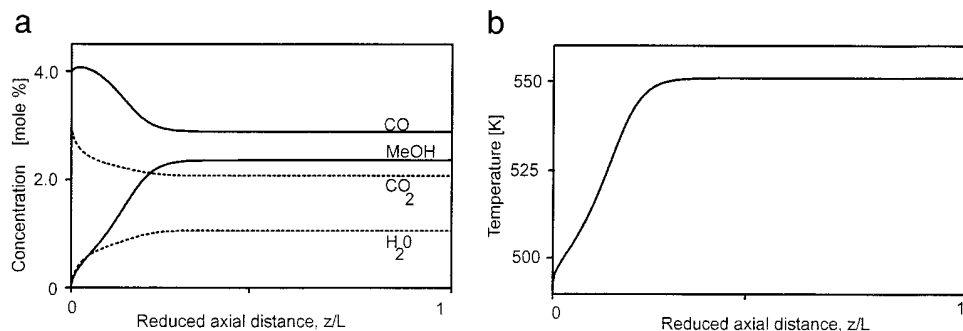


FIG. 5. (a) Simulated concentration profiles in an adiabatic reactor for the conditions specified in Table 3. (b) Simulated temperature profiles in an adiabatic reactor for the conditions specified in Table 3.

pressures indirectly influences the behavior of the pressure independent water gas shift reaction. For the 30- and 50-bar cases the reverse water gas shift equilibrium is quickly reached, and consequently, the reaction changes direction early in the bed. The slower evolution in the 15-bar case leads to a minimum in the CO₂ curve (or a maximum in the water evolution) as shown in Fig. 6c.

Varying the inlet temperature leads to an analogous behavior, as is shown in Fig. 7. For an inlet temperature of 180°C, the model predicts a very limited hydrogenation activity, a feature that was also observed in the (isothermal) experiments. At $T_{in} = 200^\circ\text{C}$, both reactions proceed at a higher rate, and consequently the reverse water gas shift changes direction earlier in the bed, as was seen upon varying the inlet pressure.

At this temperature also, a maximum is reached in the carbon conversion to methanol, at least in this specific

(overdimensioned) catalyst bed. At lower inlet temperatures, the reaction is kinetically limited, while at higher T_{in} the thermodynamic equilibria set the upper limits for the exit conversion.

Finally, it is interesting to observe the model response upon variation of the ratio of p_{CO} and p_{CO_2} at constant p_{H_2} , p_t , and temperature. Experiments of this nature were performed by Klier *et al.* (5) over a Cu/ZnO catalyst, at 75 bar and temperatures between 225 and 250°C in an isothermal reactor. As shown by the points in Fig. 8, the authors found a maximum conversion to methanol at (2:28:70) mol% of (CO₂:CO:H₂). According to Klier *et al.*, CO acts as the main source of carbon in methanol, while CO₂ ensures a certain surface oxidation level. The lower conversions at lower CO₂ concentrations are due to overreduction of the surface, while at higher CO₂ levels, this species strongly covers the active sites, decreasing catalyst activity.

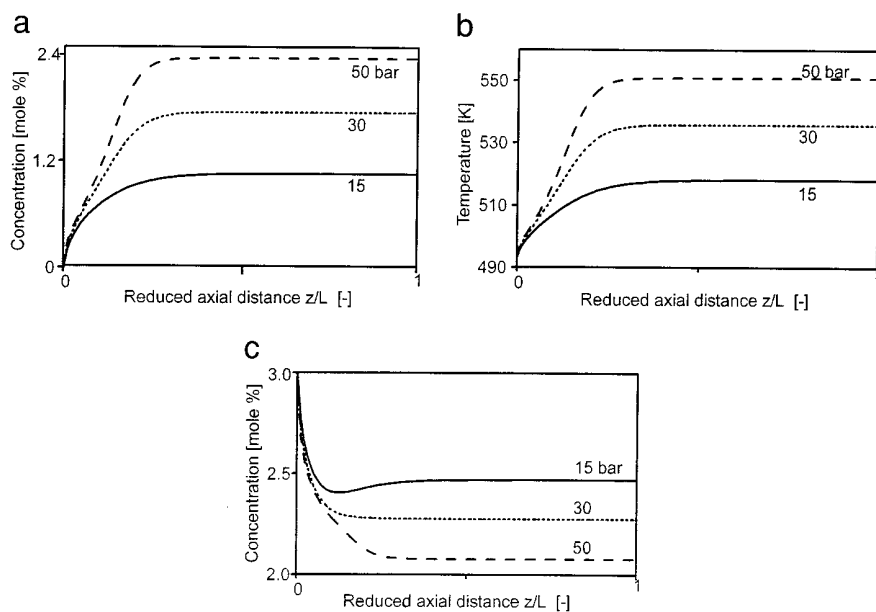


FIG. 6. (a) Simulated concentration profile of CH₃OH at various inlet pressures. (b) Simulated temperature profile at various inlet pressures. (c) Simulated concentration profile of CO₂ at various inlet pressures.

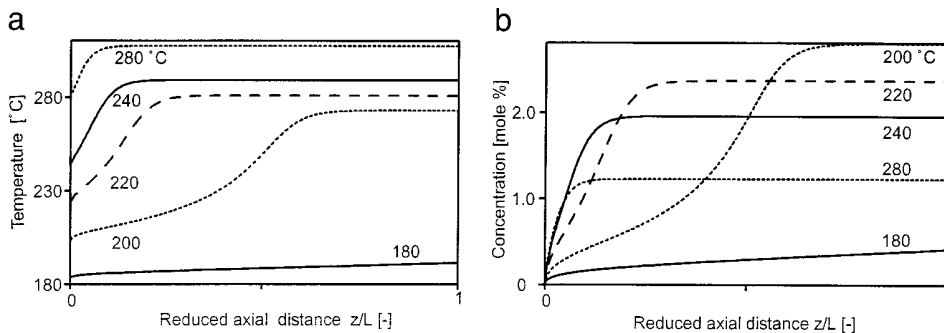


FIG. 7. (a) Simulated temperature profile at various inlet temperatures. (b) Simulated concentration profile of CH₃OH at various inlet temperatures.

The curve in Fig. 8 results from the simulations of the experiments performed by Klier *et al.* (5) at 250°C, using the current kinetic model, that was not tuned to Kliers data. It is worthy of note that the pressure as well as the composition of the gas are well outside the experimental window used to estimate the kinetic parameters. Although the present model considers only CO₂ as a precursor to methanol, it is perfectly able to qualitatively predict the evolution observed by Klier *et al.* (5). This behavior can, therefore, equally well be ascribed to a shift in the methanol equilibrium position upon the introduction of water (or CO₂), the strong adsorption of water, and the changing level of surface oxidation. In terms of the present work, the evolution is solely due to the changing oxygen (or water) concentration in the system.

In summary, these results show that the proposed model describes the influence of pressure, temperature, and gas phase composition in a physically acceptable way, even

upon extrapolation outside the experimentally applied window.

CONCLUSIONS

Based upon a detailed reaction scheme derived from literature data and own experimental work (21), a steady-state kinetic model was developed for methanol synthesis and the water gas shift reaction. Unlike some other kinetic models available in the literature, the current model effectively couples the rate of both overall reactions through the common surface oxygen intermediate.

The experiments used to determine the kinetic parameters, were performed on an industrial Cu/ZnO/Al₂O₃ catalyst at pressures between 15 and 51 bar and for temperatures varying between 180 and 280°C.

All parameters are statistically significant and satisfy each of the physico-chemical criteria postulated by Boudart

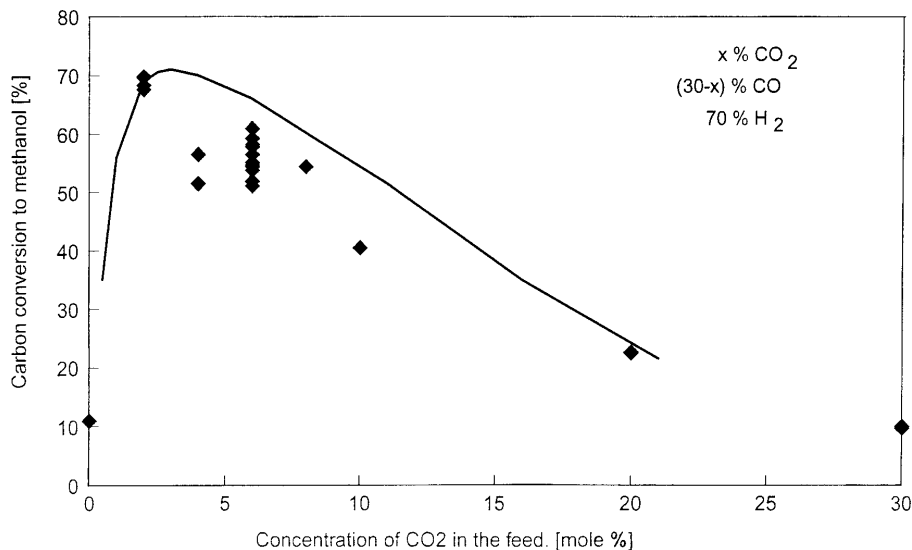


FIG. 8. Conversion to methanol for different ratios of y_{CO}/y_{CO_2} at $y_{H_2} = 0.7$, $p_t = 75$ bar; $T = 250^\circ\text{C}$; ♦, experimental results by Klier *et al.* (5); line, simulated using the current kinetic model.

(34). Furthermore, the kinetic equations describe the influence of inlet temperature, pressure, and feed composition in a physically acceptable way. The mechanistically sound foundations of the model allow for accurate predictions of catalyst behavior outside the original experimental window.

ACKNOWLEDGMENTS

The experimental assistance of V. Vanrysselberghe is gratefully acknowledged. Part of the present work was performed within the framework of the IUAP Center of Excellence Grant, provided by the Belgian Ministerie voor de Programmatie van het Wetenschapsbeleid. The authors are grateful to ICI for providing a sample of their 51-2 catalyst.

REFERENCES

- Natta, G., in "Catalysis" (P. H. Emmett, Ed.), Vol. 3, p. 349. Reinhold, New York, 1955.
- Bakemeier, H., Laurer, P. R., and Schroder, W., *Chem. Eng. Prog. Symp. Ser.* **66**(98), 1 (1970).
- Leonov, V. E., Karavaev, M. M., Tsybina, E. N., and Petrisheva, G. S., *Kinet. Katal.* **14**, 848 (1973). [in English]
- Andrew, S. P. S., "Post Congr. Symp. 7th Intern. Congr. Catal. Osaka, Japan," July 7, 1980.
- Klier, K., Chatikavanij, V., Herman, R. G., and Simmons, G. W., *J. Catal.* **74**, 343 (1982).
- McNeil, M., Schack, C., and Rinker, R., *Appl. Catal.* **50**, 265 (1989).
- Villa, P., Forzatti, P., Buzzi-Ferraris, G., Garone, G., and Pasquon, I., *Ind. Eng. Chem. Process Des. Dev.* **24**, 12 (1985).
- Graaf, G. H., Stamhuis, E. J., and Beenackers, A. A. C. M., *Chem. Eng. Sci.* **43**(12), 3185 (1988).
- Graaf, G. H., Scholtens, H., Stamhuis, E. J., and Beenackers, A. A. C. M., *Chem. Eng. Sci.* **45**(4), 773 (1990).
- Herman, R. G., Klier, K., Simmons, G. W., Finn, B. P., Bulko, J. B., and Kobyliniski, T. P., *J. Catal.* **56**, 407 (1979).
- Malinovskaya, O. A., Rozovskii, A., Ya., Zolotarskii, I. A., Lender, Yu., V., Lin, G. I., Matros, Yu. Sh., Dubovich, G. V., Popova, N. A., and Savostina, N. V., *Kinet. Katal.* **28**, 851 (1987). [Engelse vertaling]
- Mochalin, V. P., Lin, G. I., and Rozovskii, A. Ya., *Khim. Promst.* **1**, 11 (1984).
- Froment, G. F., and Bischoff, K. B., "Chemical Reactor Analysis and Design," 2nd ed., Wiley, New York, 1990.
- Chinchen, G. C., Denny, P. J., Spencer, M. S., and Whan, D. A., *Appl. Catal.* **30**, 333 (1987a).
- Rozovskii, A., Ya., *Russ. Chem. Rev.* **58**, 41 (1989).
- Chinchen, G. C., Spencer, M. S., Waugh, K. C., and Whan, D. A., *J. Chem. Soc. Faraday Trans.* **83**, 2193 (1987b).
- Nakamura, J., Canpbell, J. M., and Campbell, C. T., *J. Chem. Soc. Faraday Trans.* **86**, 2725 (1990).
- Neophytides, S. G., and Froment, G. F., *Ind. Eng. Chem. Res.* **31**, 1583 (1992).
- Ovesen, C. V., Stoltze, P., Norskov, J. K., and Campbell, C. T., *J. Catal.* **134**, 445 (1992).
- Neophytides, S. G., Marchi, A. J., and Froment, G. F., *Appl. Catal.* **86**, 45 (1992).
- Vanden Bussche, K. M., and Froment, G. F., *Appl. Catal. A* **112**, 37 (1994).
- Nonneman, L. E. Y., and Ponec, V., *Catal. Lett.* **7**, 213 (1990).
- Sheffer, G. R., and King, T. S., *J. Catal.* **115**, 376 (1989a).
- Sheffer, G. R., and King, T. S., *J. Catal.* **116**, 488 (1989b).
- Chinchen, G. C., and Spencer, M. S., *Catal. Today* **10**, 293 (1991).
- Hadden, R. A., Vandervell, H. D., Waugh, K. C., and Webb, G., *Catal. Lett.* **1**, 27 (1988).
- Copperthwaite, R. G., Davies, P. R., Morris, M. A., Roberts, M. W., and Ryder, R. A., *Catal. Lett.* **1**, 11 (1988).
- Millar, G. J., Rochester, C. H., Bailey, S., and Waugh, K. C., *J. Chem. Soc. Faraday Trans.* **88**, 2085 (1992).
- Bowker, M., Hadden, R. A., Houghton, H., Hyland, J. N. K., and Waugh, K. C., *J. Catal.* **109**, 263 (1988).
- Fujita, S., Usui, M., and Takezawa, N., *J. Catal.* **134**, 220 (1992).
- Ernst, K. H., Campbell, C. T., and Moretti, G., *J. Catal.* **134**, 66 (1992).
- Graaf, G. H., Sijtsma, P. J. J. M., Stamhuis, E. J., and Joosten, G. E. H., *Chem. Eng. Sci.* **41**, 2883 (1986).
- Marquardt, D. W., *J. Soc. Ind. Appl. Math.* **11**, 431 (1963).
- Boudart, M., *AICH EJ* **18**, 465 (1972).
- Stull, D. R., Westrum, E. F., and Sinke, G. C., "The Chemical Thermodynamics of Organic Compounds." Wiley, New York, 1969.
- Soave, G., *Chem. Eng. Sci.* **27**, 1197 (1972).